Ilka B. Bischofs, Franziska Klein, Dirk Lehnert, Martin Bastmeyer and Ulrich S. Schwarz
Filamentous Network Mechanics and Active Contractility Determine Cell and Tissue Shape

Supplementary Material

Supplementary figures

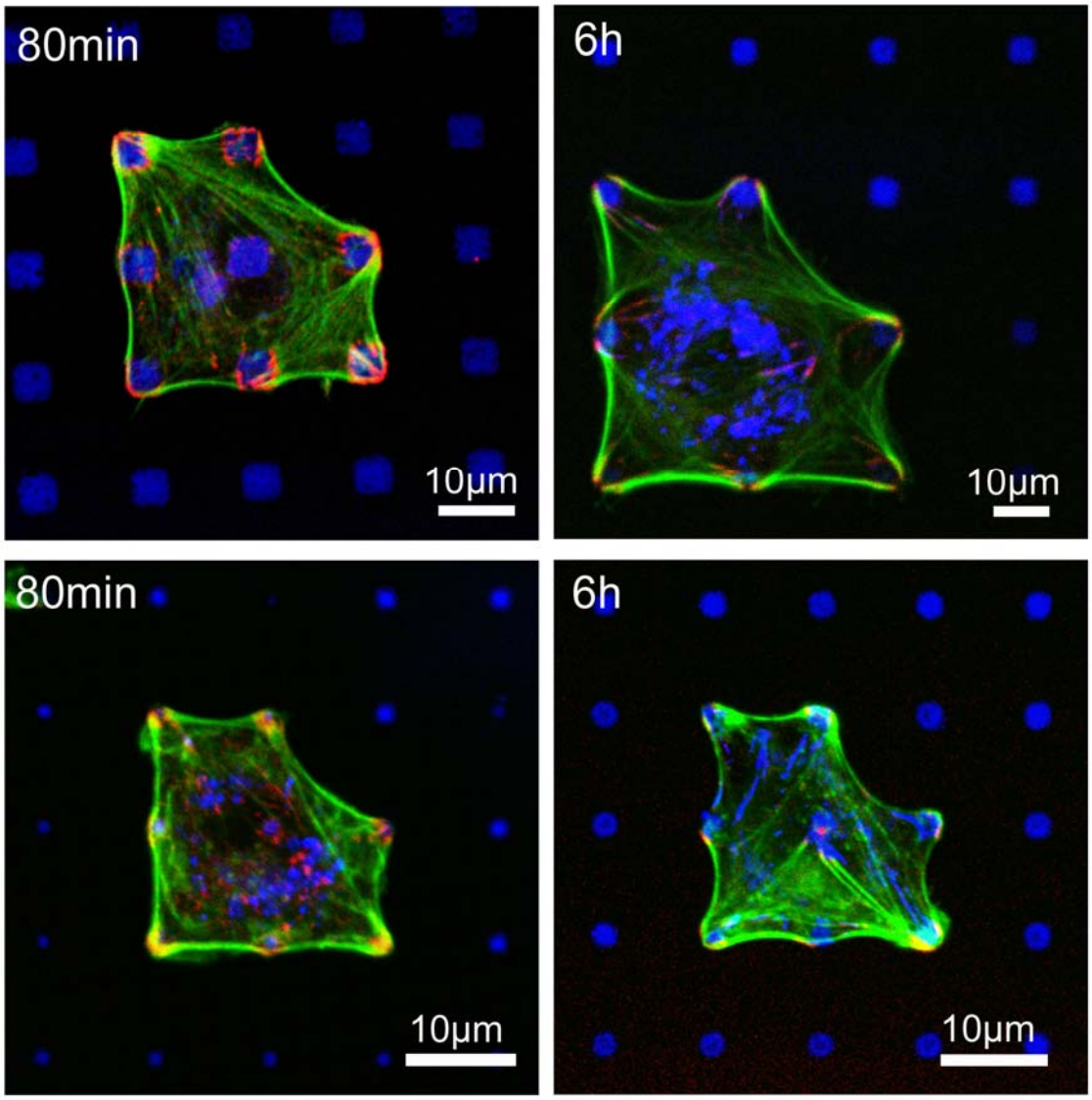

Figure S1: Dynamics of cell adhesion

BRL- (upper row) and B16-cells (lower row) were cultured on patterned substrates in serum-free medium, fixed and stained for actin (green), paxillin (red) and fibronectin (blue). Under these culture conditions, cell migration is largely reduced and cell spreading completed after one hour. A comparision of two cells cultured for 80 min with two cells cultured for 6 hours shows no differences in typical arc structures, indicating that the cells have established an almost stationary cell shape.

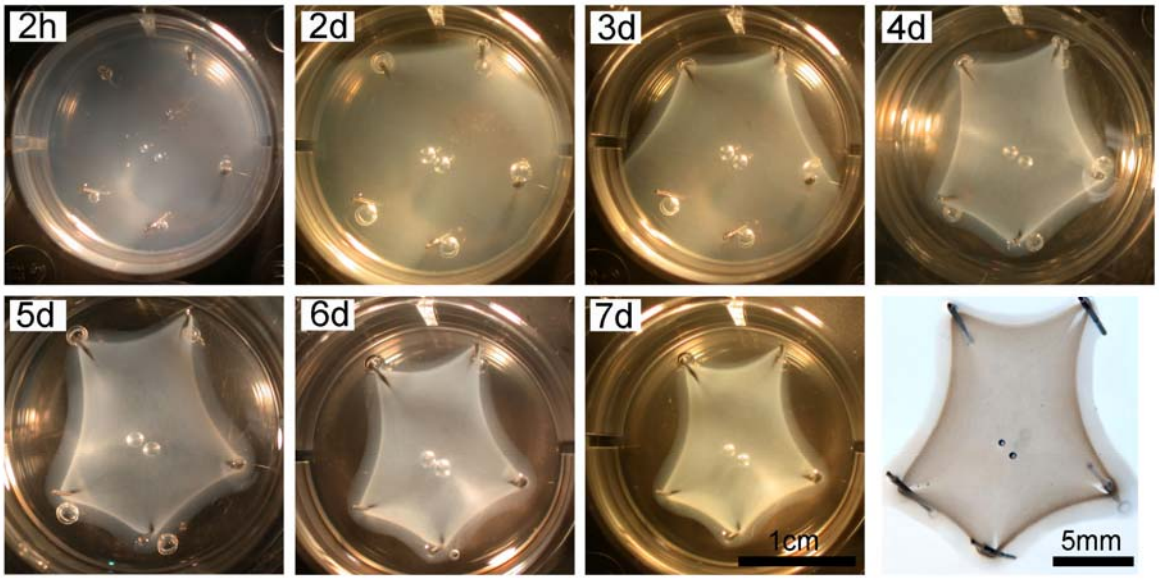

Figure S2: Dynamics of the tissue model

Time series for a tissue model with embryonic fibroblasts and rat tail collagen. The image shown in Fig. 2A (also last image here) is the fixed version of the image at day 7 in the time series. After 2h, cells and collagen are still a uniform dispersion. Steel needles attached to the bottom of the dish provide mechanical resistance to cellular forces. After a few days, gel shape develops in response to the geometry of the pinning points. Cellular contraction is sufficiently large to lead to fracture in the gel close to the pinning points.

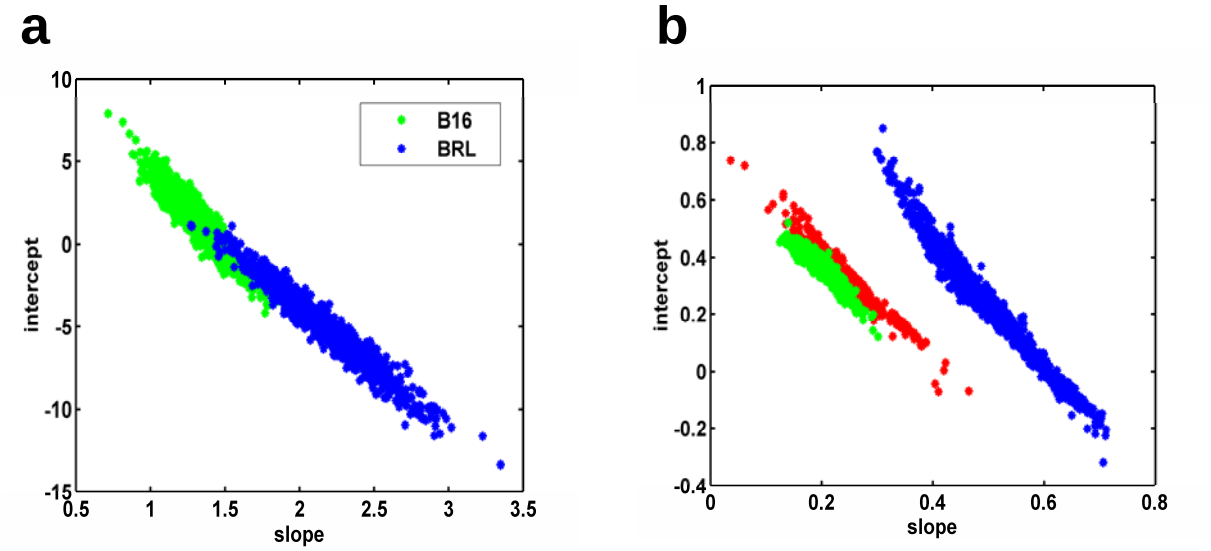

Figure S3: Parameter distribution for linear fits obtained from bootstrapping

(a) Slope and intercept of a linear fit to the R-d-correlation from Fig. 3C of BRL (blue) and B16 cells (green). The difference between the R-d relationships is not significant since the parameter distributions do overlap. (b) Slope and intercept of a linear fit to the <R/d>(S) relationship from Fig. 7E for BRL control cells (blue), blebbistatin treated cells (red) and Y27632 treated cells (green). The difference between the two inhibition protocols is not significant. The correlation of the control cells is significantly different from the inhibited cells.

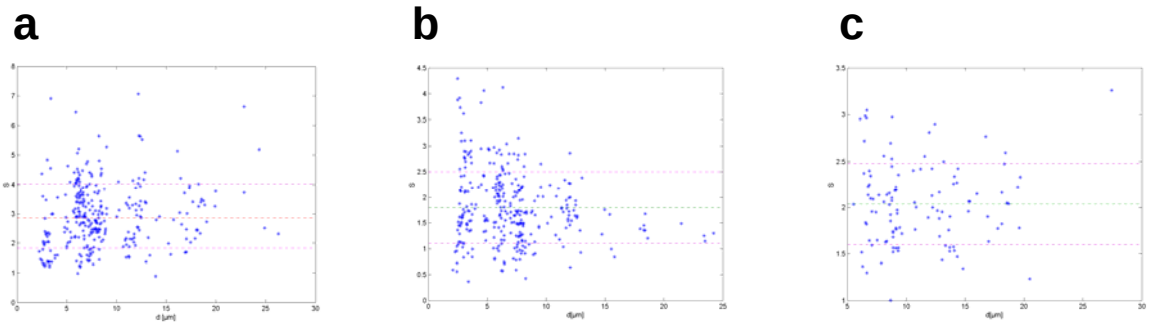

Figure S4: A longer fiber is not a stronger fiber

Correlation coefficients C between spanning distance d and arc strength S are persistently small. (a) Control BRL: C=0.16. (b) Y-27632-treatment: C=-0.21. (c) Blebbistatin-treatment: C=0.04.

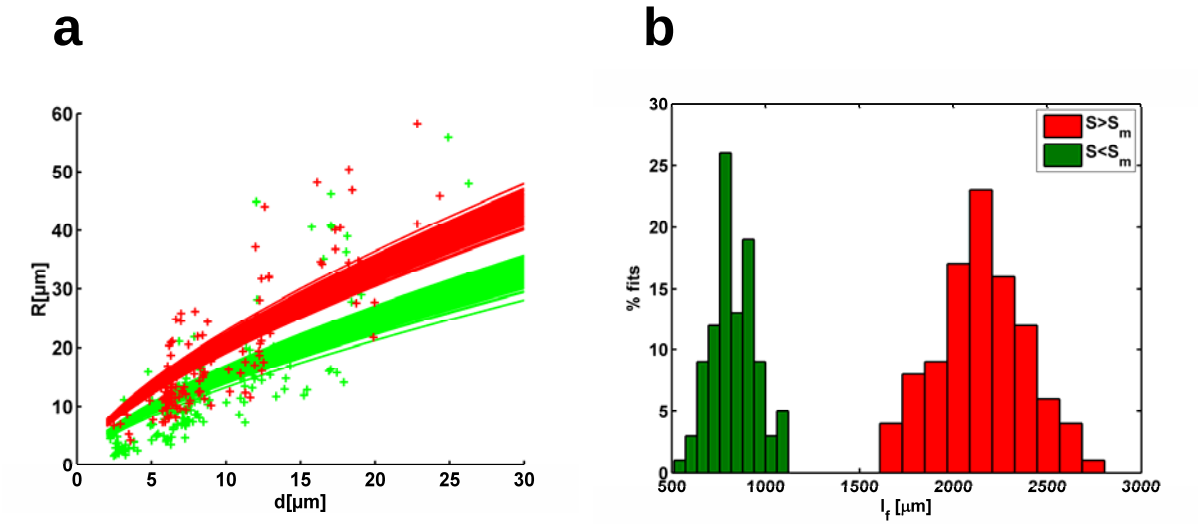

Figure S5: Variation in arc strength

(a) R-d relations for weak (green, $S<S_m$) and strong (red, $S>S_m$) arc subpopulations. Lines show 100 bootstrap fits to the EC-model for the respective subpopulations. (b) Distribution of the fit parameter l_f for weak (green) and strong (red) arcs. Weaker arcs lead to statistically significant smaller values of l_f than strong arcs. Thus arc strength variations contribute to the spread in the R(d)-data for BRL-cells shown in Fig. 3C.

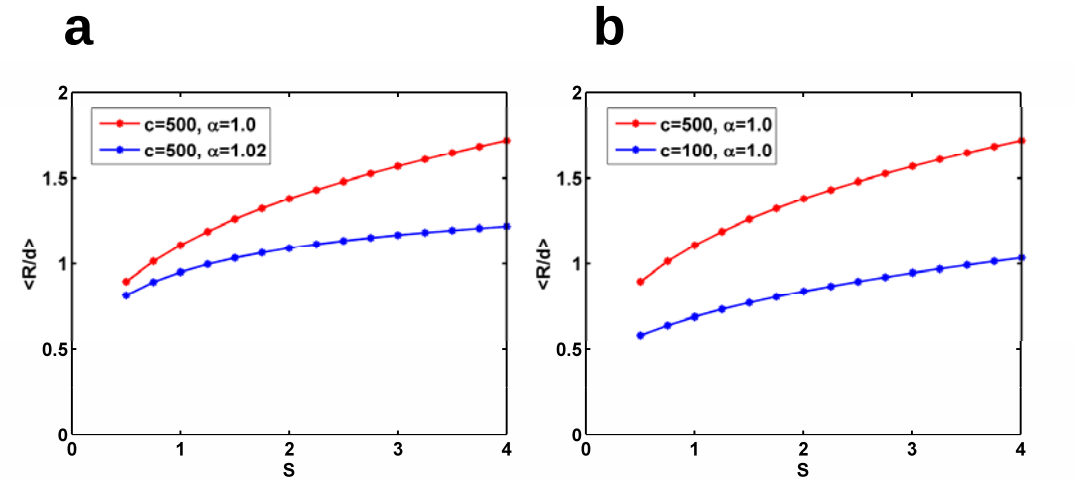

Figure S6: Theoretical effect of arc strength variation

Model prediction for the variation of the averaged normalized arc radius <R/d> with arc strength S. Here we assume EA=cS with c=500 as estimated from the control data. The red line denotes the prediction of the model for BRL control cells in both cases. The blue line is the model prediction for inhibited cells. Experimental results are shown in Fig. 7E. (a) Model prediction with TC-model when inhibition causes an increase of fiber resting length α due to tension relaxation. (b) Model prediction by an alternative scenario in which additional elastic effects not captured by the arc strength cause an effective reduction in c without changing α.

Tension-elasticity model

Computer Simulations

In the following, the model is explained in terms of cell shape, but the same theory also applies to tissue shape as explained in the main text. Our computer simulations model the cell as an actively contracting two-dimensional cable network. We first generate nodes and links for a tension-free reference state. For regular networks, nodes are positioned on a square lattice, with each internal node linked to four adjacent nodes. For irregular networks, nodes were distributed at random, but with a required minimal distance to neighbouring nodes, such that internal nodes are typically linked to five to six neighbours. Each link represents a mechanical network element: in a fully elastic network each link denotes a harmonic spring with a linear force-extension relationship, while in a cable network, each link represents a cable which responds linearly to stretch but yields to compression. The contractile activity within the network is modelled as a homogenous distribution of pairs of opposing body forces that act on opposite nodes of a connecting link. This rule is applied to all links in the network. We then use a steepest descent algorithm to relax the network into mechanical equilibrium.

Effective Contour Model

(a) Mechanical Equilibrium

The shape of a cell adhering to a flat rigid substrate is mainly represented by its two-dimensional contour. The existence of circular arcs suggests that cell shape is determined by an effective surface tension σ, which acts to decrease cell area, and an effective line tension λ, which acts to decrease contour length between neighbouring sites of adhesion. Then the shape of a free part of the contour results from the local force balance between surface tension and line tension:

$$\sigma\vec{n} = \lambda\frac{d\vec{t}}{ds} = \frac{\lambda}{R}\vec{n}\,, \qquad \text{(Eq. 1)}$$

where $\vec{n}$ and $\vec{t}$ are normal and tangential vectors to the cell contour, respectively, s is the contour coordinate and R the radius of curvature. Therefore, the contour is a circular arc with radius $R=\lambda/\sigma$. This equation is the 2D analogue to the 3D Laplace law for the radius of a pressurized spherical (soap) bubble under surface tension in mechanical equilibrium.

(b) Adhesion Constraints and R(d)-relationship

Although mechanical equilibrium between surface and line tension explains the experimental finding of constant radius R along the arcs, it cannot explain the additional experimental finding that radius R depends on the spanning distance d. This suggests an elastic effect as elasticity depends on absolute distances, in this case the spanning distance between the adhesion points anchoring the cell contour to the substrate. We therefore hypothesize that the effective line tension results from elastic strain along the cell contour. In the framework of linear elasticity theory:

$$\lambda = EAu\,, \qquad \text{(Eq.2)}$$

where E is the three-dimensional Young modulus of the strained material and A is its cross-sectional area; therefore EA is the one-dimensional Young modulus or rigidity of the contour. The variable u is the relative deformation (strain) given by

$$u = \frac{L - L_0}{L_0}, \quad \text{(Eq.3)}$$

where L is the actual arc length and L_0 the resting length, that is the length the fiber relaxes to if all constraints were removed. Combining Eq.1 and Eq.2 we obtain:

$$R = l_f u\,, \qquad \text{(Eq.4)}$$

where l_f=EA/σ is a length scale set by the ratio of rigidity and surface tension. In general the contour strain u depends on additional conditions set by the adhesion constraints. Thus line tension is not a constant parameter, but depends on adhesion geometry. As both l_f and u are the same along a given arc, this theory explains both why arcs have constant radii (local mechanical equilibrium between surface and line tension) yet depend on spanning distances d (line tension depends on strain). In detail, the adhesion geometry imposes the following boundary condition obtained from simple trigonometry (Fig. 3B) since the contour is fixed at the adhesion points separated by a distance d:

$$R = \frac{d}{2\sin\left(\frac{L}{2R}\right)}\,. \qquad \text{(Eq.5)}$$

This can be inverted to yield

$$L = 2R\arcsin\left(\frac{d}{2R}\right). \quad \text{(Eq.6)}$$

An additional constraint is set by the conditions characterizing the tension free reference state of the contour, which here is represented by the resting length L_0 of the fiber. As this quantity cannot be measured experimentally, we have to make some reasonable assumption. A natural choice is to assume that the resting length of the fiber scales with the spanning distance d, i.e.

$$L_0 = \alpha d, \qquad \text{(Eq.7)}$$

where α is a dimensionless rest length parameter. Combining Eqs.(3,4,6,7), we therefore arrive at an implicit equation for the arc radius R:

$$R = l_f u = l_f \frac{L - L_0}{L_0} = l_f\left(\frac{2R}{L_0}\arcsin\left(\frac{d}{2R}\right) - 1\right) = l_f\left(\frac{2R}{\alpha d}\arcsin\left(\frac{d}{2R}\right) - 1\right) \quad \text{(Eq.8)}$$

This implicit equation defines the desired relation R(d).

Elasticity and Tension Control

(a) Model Predictions

The exact nature of the distance dependence of the arc radius R(d) emerging from Eq.8 depends only on two parameters, the length scale scale l_f characterizing the mechanical fiber response to tension and the resting length parameter α. Each parameter is linked to an independent control mode, which we term *elasticity control* (EC) and *tension control* (TC), respectively.

Elasticity control results from structural changes in the contour fiber altering its mechanical rigidity EA. The structural properties of actin bundles are strongly regulated and are adapted quickly to both extra- and intracellular changes. A decrease in rigidity of the contour EA, i.e. a mechanically weaker fiber, results in a decrease of l_f, which in turn leads to a decrease in arc radius R, because now the same surface tension σ is pulling in a mechanically weaker contour.

Tension control is mediated by changes in the rest length parameter α, which might result from actomyosin contractility which can dynamically change the rest length of the fiber bundle by sliding actin filaments relatively to each other. As α increases, the fiber relaxes and arc radius R decreases, because more extra length can be drawn in by the surface tension σ.

There are three different regimes for R(d) as α is varied:

1. If $\alpha<1$, the fiber is under strain $u_p=(1-\alpha)/\alpha$ even if no surface tension σ is pulling the cell contour inward. This results in a finite intercept radius $R(0)=R_{min}$ as the adhesion distance approaches 0 and a superlinear increase of R with d. For small values of d/R, a detailed mathematical analysis gives:
$$R = \frac{l_f(1-\alpha)}{\alpha} + \frac{\alpha d^2}{24 l_f (1-\alpha)^2} \quad \text{(Eq.9)}$$
2. If $\alpha=1$, the fiber is straight, but without strain in the absence of surface tension σ. This results in a R-d-correlation which increases more weakly than linear with d. For small values of d/R, the mathematical analysis gives:
$$R = \left(\frac{l_f}{24}\right)^{\frac{1}{3}} d^{\frac{2}{3}} \qquad \text{(Eq.10)}$$
3. If $\alpha>1$, the tension free fiber is longer than d and has extra length stored in the contour. In this case, an infinitesimally small amout of tension σ will be sufficient to induce a strain free arc radius $R_{max}(\alpha,d)$ for each d even for a rigid fiber ($l_f \mapsto \infty$), which simply corresponds to a circular arc of length L_0 with a secant of d. The formula for $R_{max}(\alpha,d)$ results from Eq.6 with $L=L_0=\alpha d$ and results in a roughly linear R-d-relationship. Any additional amount of tension σ for a fiber with finite rigidity or any softening of the fiber will then result in smaller radii. Hence as l_f increases and the strain in the fiber decreases, R(d) asymptotically approaches the limit $R_{max}(\alpha,d)$.

(b) Comparison with experiment

The tension-elasticity model was extensively used for fits to the experimental results. The fit parameters were estimated from a non-linear least square fit to the respective implicit model equations and statistically analysed with bootstrapping. However, allowing both l_f and α to be free fit parameters leads to an ill-conditioned problem. Ill-conditioned fitting problems often indicate that one fit parameter can be eliminated. We therefore separately considered two scenarios defined by:

Elasticity control (EC):	l_f is the only fit parameter. We choose $\alpha=1$ to avoid constraining the fit by a α−determined R_{max} asymptote. The determined l_f values denote a lower bound of the full model.
Tension control (TC):	α is the only fit parameter. For this purpose we consider the asymptotic rigid fiber case $l_f \mapsto \infty$. The determined fit values denote upper bounds of the full model.

Indeed we find that both single parameter models (EC and TC) lead to satisfactory fitting results suggesting that the experimental data does not constrain the model enough to distinguish unambiguously between different scenarios.

Arc Strength Variation

(a) Model Predictions

In order to derive model predictions for variations in arc strength, we assume that the rigidity EA of the fiber scales linear with arc strength S, such that:
$$l_f = \frac{EA}{\sigma} = cS, \qquad \text{(Eq.11)}$$

where c is a function of the surface tension σ. For constant experimental conditions we may assume that c is constant and all variations in l_f are caused by variations in arc strength S. For this situation our model predicts that increases in arc strength S will cause decreased arc radii via elasticity control (EC-model). Note that for a very large average l_f and $\alpha>1$, R will approach its asymptotic value R_{max} and hence R will become insensitive to arc strength variations. Hence a lack of correlation between S and R would indicate that shape is entirely controlled by rest length variation (TC-model).

(b) Comparison with Experiment

Experimentally arc strength S in BRL cells does vary from arc to arc and this variation is correlated with the arc radius R. Experimentally a 2-3 fold variation in S as measured for BRL cells has a pronounced effect on R, thus favouring a model involving elasticity as a mean to control cellular line tension. This also implies that the spread in R(d) for at a given distance d is in part due to a heterogeneous arc strength S varying from arc to arc. To further analyze this effect, we split arcs in two equally large groups of strong ($S > S_m$) and weak ($S < S_m$) arcs according whether their strength exceeds the median S_m of the arc strength distribution or not. The fits to the respective subpopulations according to EC-model to the data show that the strong arc subpopulation has a statistically significant larger l_f values than weak arc subpopulation (Fig. S5). We have also considered the possibility that arc strength S varies with adhesion distance d per se and thus indirectly might cause a correlation of arc radius R with adhesion distance d, independent from the boundary and initial condition effects discussed in the tension-elasticity model. However, the experimentally determined correlation coefficients are consistently small for all experimental conditions ($C<0.2$, Fig. S4). This suggests that there exist no global correlation between arc strength and arc distance that would be sufficient to explain the observed strong positive correlation between R and d in the experiments.

Motor Inhibition

Inhibition of motor tension has manifold effects on cell shape and affects both line and surface tension. In addition it involves mechanosensitive feedback reactions that couple tension to structural reinforcement of the boundary. Hence a priori predictions are very difficult. Experimentally we find that motor inhibition causes a structural weakening of the arcs as quantified by significantly lower average arc strength S. This structural weakening is also reflected in the R(d) correlation since arc strength decreases considerably under motor inhibition. This raises the question whether cell shape is entirely controlled by arc strength variations. If this was the case, one would expect that structurally similar arcs, i.e. arcs with the same S, have the same radii for a given distance d regardless whether cells are motor inhibited or not. In order to obtain sufficient statistics we computed a distance normalized arc radius by computing the average of <R/d> as a function of arc strength S.

(a) Model Predictions

As motors are inhibited, tension in the fiber might relax, which effectively increases the rest length of the fiber, i.e. α increases (TC-model). We therefore computed the theoretical predictions for <R/d>(S) for the different α regimes using Eqs.(8,11). The numerical solutions approach the analytical predictions emerging from combining Eqs.(9-11). Assuming c to be constant, our theoretical model predicts that the effective sloping of <R/d> becomes shallower with S as α increases. As mentioned before, c may not be constant under inhibition. Indeed our model shows that a reduction of c without changing α effectively could cause a similar effect as variations in α keeping c fixed (Fig. S6).

(b) Comparison with Experiment

We determined the functional relationship between <R/d> and S experimentally by median averaging over at least five R-d data points in a given interval of $\Delta S=0.25$ (Fig. 7E). For BRL cells under control conditions we may estimate c from the fits estimating l_f from the R(d)-correlation. Keeping $\alpha=1$, l_f for BRL cells was determined from fitting to lie between [500, 2500]. We therefore chose $c = l_f /S=500$. Then the emerging theoretical results obtained for the dependence of the normalized radius <R/d> on the arc strength S are in reasonable quantitative agreement with the experimental observations. Under inhibition of contractility <R/d>-values at the same arc strength S are considerably smaller compared to control cells and the effective sloping of R/d(S) is considerably shallower. This implies that additional effects must control arc radius other than arc strength. Our theoretical model predicts that tension control mediated an increase in fiber resting length under tension relaxation could explain this finding. Keeping c=500 the effective sloping behaviour predicted by our model becomes shallower with S as α increases. Hence, there is good qualitative agreement between the experimental observations with the model assuming an increase in effective fiber rest length under relaxed tension.

The alternative scenario suggested by our model, namely a reduction of c, seems less likely. Motor inhibition is expected to reduce the surface tension to baseline levels determined by plasma membrane tension. This effect tends to actually *increase* c rather than decrease it. Hence myosin-dependent additional elastic effects, not captured by our arc strength measurement, would have to overcome the reduction in σ and cause an overall decrease in c. Note that this overcompensation must decrease l_f by at least *one order of magnitude*. This seems unlikely. We therefore conclude that both elastic and tension control determine line tension and thus cell shape.